Exclusive Photoproduction of Quarkonia in QCD at NLO

Lech Szymanowski

National Centre for Nuclear Research (NCBJ)
Warsaw, Poland

IHP, Paris, 24-25 September 2015

based on Eur. Phys. J. C 34 (2004) 297, Err.: C75 (2015) 2, 75

in collaboration with D. Yu. Ivanov (Institut of Mathematics, Novosibirsk)
G. Krasnikov (St. Petersburg University),
J. Wagner (NCBJ, Warsaw),

Content:

- Method of calculation
- Comparison with data and phenomenolgy

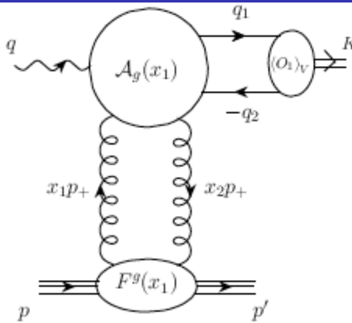

$$\Delta = p' - p\,, \quad P = \frac{p+p'}{2}\,, \quad t = \Delta^2\,,$$

$$(q-\Delta)^2 = K^2 = M^2\,, \quad \zeta = \frac{M^2}{W^2}\,.$$

$$q = \frac{(W^2 - m_N^2)}{2(1+\xi)W}\, n_-\,,$$

$$p = (1+\xi)W\, n_+ + \frac{m_N^2}{2(1+\xi)W}\, n_-\,,$$

$$p' = (1-\xi)W\, n_+ + \frac{(m_N^2 + \mathbf{\Delta}^2)}{2(1-\xi)W}\, n_- + \Delta_\perp\,,$$

$$\Delta = -2\,\xi\, W\, n_+ + \left(\frac{\xi\, m_N^2}{(1-\xi^2)W} + \frac{\mathbf{\Delta}^2}{2\,(1-\xi)W}\right) n_-$$

$$+\Delta_\perp\,. \qquad ($$

Factorisation in LO

- quarkonium vertex:

$$v_i(q_2)\,\bar{u}_j(q_1) \to \frac{\delta_{ij}}{4N_c}\left(\frac{\langle O_1\rangle_V}{m}\right)^{1/2} \not{\epsilon}^*_V\,(\not{K}+M)\,.$$

- Factorised amplitude

$$\mathcal{M} = \left(\frac{\langle O_1\rangle_V}{m}\right)^{1/2} \sum_{p=g,q,\bar{q}} \int_0^1 \mathrm{d}x_1\, A^p_{\mathrm{H}}(x_1,\mu_{\mathrm{F}}^2)\,\mathcal{F}^p_\zeta(x_1,t,\mu_{\mathrm{F}}^2)\,.$$

$$x_1 = \frac{x+\xi}{1+\xi}\,, \quad x_2 = \frac{x-\xi}{1+\xi}\,.$$

Factorisation in LO

- gluonic GPDs in the leading twist 2

$$
\begin{aligned}
F^g(x,\xi,t) \\
&= \frac{1}{(Pn_-)} \int \frac{\mathrm{d}\lambda}{2\pi} \mathrm{e}^{\mathrm{i}x(Pz)}\, n_{-\alpha} n_{-\beta} \\
&\qquad \times \langle p'| G^{\alpha\mu}\left(-\frac{z}{2}\right) G_\mu^\beta\left(\frac{z}{2}\right) |p\rangle\Big|_{z=\lambda n_-} \\
&= \frac{1}{2(Pn_-)} \Big[\mathcal{H}^g(x,\xi,t)\, \bar{u}(p')\, \not{n}_- u(p) \\
&\qquad + \mathcal{E}^g(x,\xi,t)\, \bar{u}(p') \frac{\mathrm{i}\sigma^{\alpha\beta} n_{-\alpha}\Delta_\beta}{2\, m_N} u(p) \Big]
\end{aligned}
$$

- in the axial gauge

$$
\begin{aligned}
&\int \frac{\mathrm{d}\lambda (Pn_-)}{2\pi} \mathrm{e}^{\mathrm{i}x(Pz)} \langle p'| A_\mu^a\left(-\frac{z}{2}\right) A_\nu^b\left(\frac{z}{2}\right) |p\rangle\Big|_z \\
&= \frac{\delta^{ab}}{N_c^2 - 1} \left(\frac{-g_{\mu\nu}^\perp}{2}\right) \frac{F^g(x,\xi,t)}{(x-\xi+\mathrm{i}\varepsilon)(x+\xi-\mathrm{i}\varepsilon)} .
\end{aligned}
$$

$z = \lambda n_-$

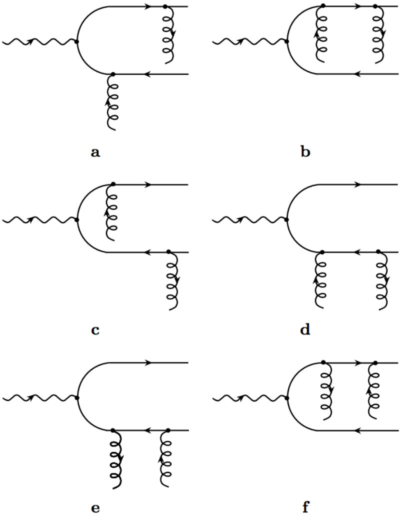

Fig. 2a–f. The hard-scattering amplitude at LO

Factorisation in LO

- Results in LO

$$\mathcal{M} = \frac{4\pi\sqrt{4\pi\alpha}\, e_q (e_V^* e_\gamma)}{N_c\, \xi} \left(\frac{\langle O_1 \rangle_V}{m^3} \right)^{1/2} \int\limits_{-1}^{1} dx \left[T_g(x,\xi)\, F^g(x,\xi,t) + T_q(x,\xi) F^{q,S}(x,\xi,t) \right]$$

$$F^{q,S}(x,\xi,t) = \sum_{q=u,d,s} F^q(x,\xi,t)$$

Factorisation in LO

- Results in LO

$$\mathcal{M} = \frac{4\pi\sqrt{4\pi\alpha}\, e_q (e_V^* e_\gamma)}{N_c\, \xi} \left(\frac{\langle O_1\rangle_V}{m^3}\right)^{1/2} \int_{-1}^{1} dx \left[T_g(x,\xi)\, F^g(x,\xi,t) + T_q(x,\xi) F^{q,S}(x,\xi,t) \right]$$

$$F^{q,S}(x,\xi,t) = \sum_{q=u,d,s} F^q(x,\xi,t)$$

$$T_g(x,\xi) = \frac{\xi}{(x-\xi+\mathrm{i}\varepsilon)(x+\xi-\mathrm{i}\varepsilon)} \mathcal{A}_g\left(\frac{x-\xi+\mathrm{i}\varepsilon}{2\xi}\right)$$

$$T_q(x,\xi) = \mathcal{A}_q\left(\frac{x-\xi+\mathrm{i}\varepsilon}{2\xi}\right). \qquad (2$$

$$\mathcal{A}_g^{(0)}(y) = \alpha_S(1+\epsilon)\,,$$

$$\mathcal{A}_q^{(0)}(y) = 0\,.$$

Hard-scattering amplitudes at NLO

- Method of calculation: unitarity and dispersion relations

$$\tilde{s} = x_1 s \qquad \zeta = \frac{M^2}{W^2}$$

$$y = \frac{\tilde{s} - M^2}{M^2} = \frac{x_2}{\zeta} = \frac{x - \xi}{2\xi}$$

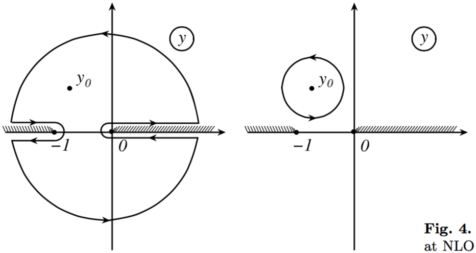

Fig. 4. The analytical properties of the partonic amplitudes at NLO in the complex plane of $y = x_2/\zeta$

$$\tilde{s} \leftrightarrow \tilde{u} \qquad \Rightarrow \qquad y \leftrightarrow -(1+y)$$

Hard-scattering amplitudes at NLO: Quark CF

- unsubstracted dispersion relation

$$\mathcal{A}_q^{(1)}(y) = \frac{1}{\pi}\int_0^{\infty} \mathrm{d}z \, \mathrm{Im}\, \mathcal{A}_q^{(1)}(z) \left(\frac{1}{z-y} - \frac{1}{z+y+1} \right)$$

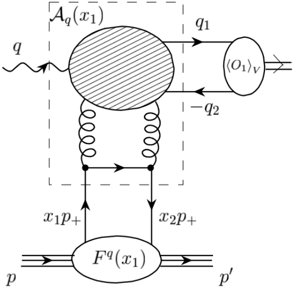

Fig. 3. The light quark contribution to heavy meson photo-production

Hard-scattering amplitudes at NLO: Quark CF

- non-polarised quark GPDs

$$
\begin{aligned}
&F^q(x,\xi,t) \\
&= \frac{1}{2}\int \frac{\mathrm{d}\lambda}{2\pi} \mathrm{e}^{\mathrm{i}x(Pz)} \, \langle p'|\bar{q}\left(-\frac{z}{2}\right) \not{n}_- q\left(\frac{z}{2}\right)|p\rangle\Big|_z \\
&= \frac{1}{2(Pn_-)}\Big[\mathcal{H}^q(x,\xi,t)\,\bar{u}(p')\,\not{n}_- u(p) \\
&\qquad + \mathcal{E}^q(x,\xi,t)\,\bar{u}(p')\frac{\mathrm{i}\sigma^{\alpha\beta}n_{-\alpha}\Delta_\beta}{2\,m_N}u(p)\Big]
\end{aligned}
$$

Hard-scattering amplitudes at NLO: Quark CF

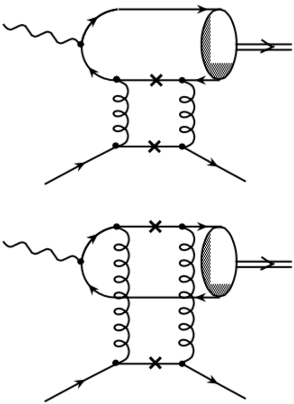

Fig. 5. The $\tilde{s}$-channel cut diagrams for the quark amplitude

Hard-scattering amplitudes at NLO: Quark CF

$$\mathcal{A}_q^{(1)}(y) = \frac{\alpha_S^2 C_F}{(4\pi)^{1+\epsilon}\Gamma(1+\epsilon)} \left(\frac{4m^2}{\mu^2}\right)^{\epsilon} \mathcal{I}_q(y)$$

$$\begin{aligned}
\mathcal{I}_q(y) = {} & \frac{2}{\epsilon}(1+2y)\left(\frac{\ln(-y)}{1+y} - \frac{\ln(1+y)}{y}\right) \\
& - \pi^2 \frac{13\,(1+2y)}{24\,y\,(1+y)} + \frac{4\ln 2}{1+2y} + 2\frac{\ln(-y)+\ln(1+y)}{1+2y} \\
& + 2(1+2y)\left(\frac{\ln^2(-y)}{1+y} - \frac{\ln^2(1+y)}{y}\right) \\
& + \frac{3-4y+16y(1+y)}{2y(1+y)}\mathrm{Li}_2(1+2y) \\
& - \frac{7+4y+16y(1+y)}{2y(1+y)}\mathrm{Li}_2(-1-2y)\,,
\end{aligned}$$

where

$$\mathrm{Li}_2(z) = -\int_0^z \frac{\mathrm{d}t}{t}\ln(1-t)\,.$$

Hard-scattering amplitudes at NLO: Gluon CF

- substracted dispersion relation

$$\mathcal{A}_g^{(1)}(y) - \mathcal{A}_g^{(1)}(0) = \frac{1}{\pi} \int_0^\infty \mathrm{d}z \, \mathrm{Im}\, \mathcal{A}_g^{(1)}(z)$$

$$\times \left(\frac{y}{z(z-y)} - \frac{y}{(z+y)(z+y+1)} \right) .$$

- three s-channel cuts: $\bar{Q} \; - \; Q, \quad \bar{Q} \; - \; g, \quad Q \; - \; g$

- $\bar{Q}\,Q$ cut

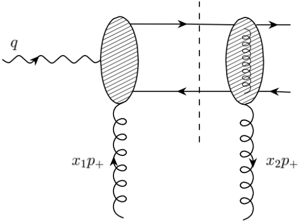

Fig. 6. The contribution of the $\bar{Q}Q$ intermediate state to the gluonic amplitude

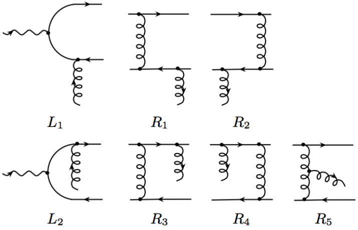

Fig. 7. The left and the right effective vertices for the $\bar{Q}Q$ cut

Hard-scattering amplitudes at NLO: Gluon CF

- $\bar{Q}\, g$ cut

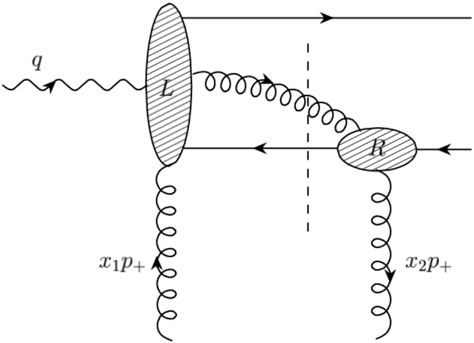

Fig. 8. The contribution of the $\bar{Q}g$ intermediate state to the gluonic amplitude

Hard-scattering amplitudes at NLO: Gluon CF

- $\bar{Q}\ g$ cut cntd

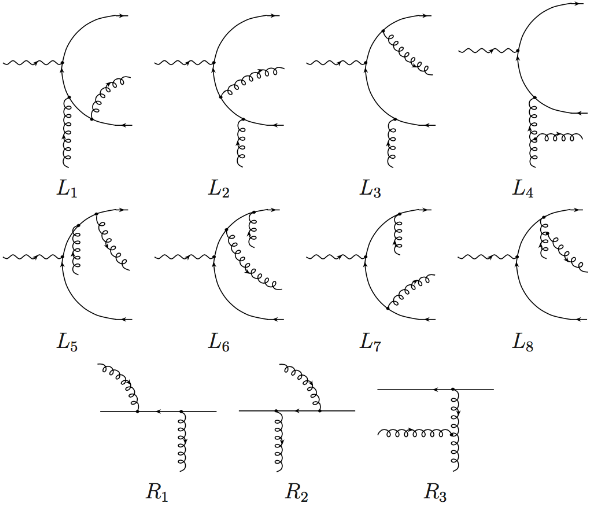

Figure 9: The left and the right effective vertices for the $\bar{Q}g$-cut.

Hard-scattering amplitudes at NLO: Gluon CF

- substracted dispersion relation

$$\mathcal{A}_g^{(1)}(y) - \mathcal{A}_g^{(1)}(0) = \frac{1}{\pi}\int_0^\infty \mathrm{d}z\, \mathrm{Im}\, \mathcal{A}_g^{(1)}(z)$$

$$\times \left(\frac{y}{z(z-y)} - \frac{y}{(z+y)(z+y+1)} \right) .$$

- three s-channel cuts: $\bar{Q} - Q$, $\bar{Q} - g$, $Q - g$

- determination of the subtraction constant $\mathcal{A}_g^{(1)}(0)$:

  Low theorem from QED applied to QCD for soft gluon with $x_2 \to 0$

- renormalization

Hard-scattering amplitudes at NLO: Gluon CF

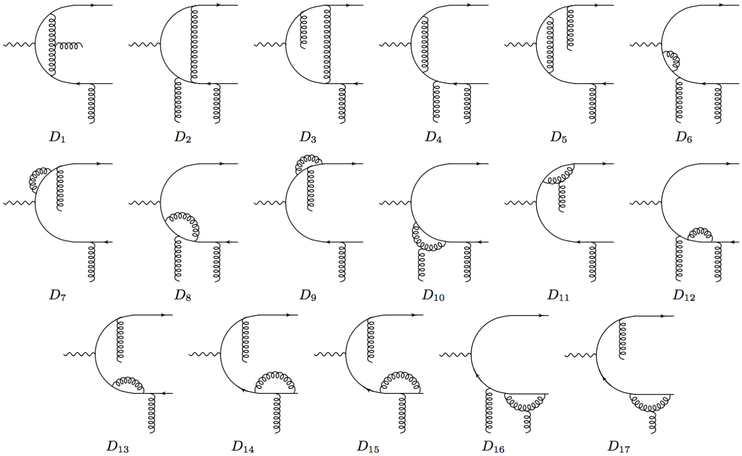

Fig. 10. Diagrams D_i, describing the radiation of a soft gluon from the on-shell antiquark line

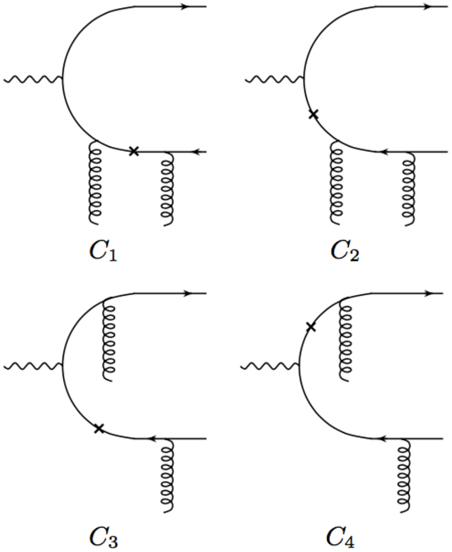

Fig. 11. Mass counterterm diagrams which have an antiquark pole in the soft gluon limit

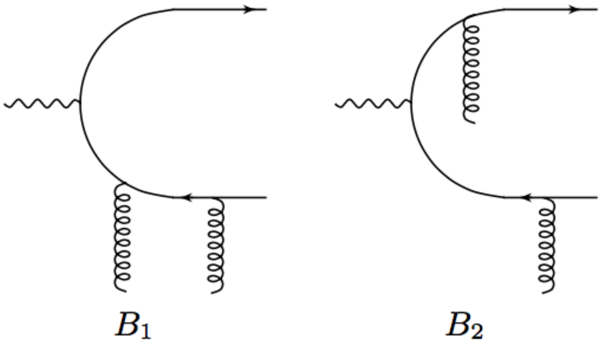

Fig. 12. LO antiquark pole diagrams

Table 1. Contributions to $\mathcal{I}_g(0)$ of diagrams $D_1, \ldots, D_{11}$

Diagram	ϵ^{-2}	ϵ^{-1}	ϵ^{0}
D_1^z	$-\frac{3}{8}(c_1 - c_2)$	$-\frac{3}{8}(c_1 - c_2)$	$(c_1 - c_2)\left(\frac{\pi^2}{16} + \frac{5\ln(2)}{4}\right)$
D_1^{add}	$-\frac{3}{8}(c_1 - c_2)$	$-\frac{3}{8}(c_1 - c_2)$	$(c_1 - c_2)\left(-\frac{1}{2} + \frac{\pi^2}{4} + \frac{7\ln(2)}{2}\right)$
D_2^z	0	$-\frac{1}{4}c_2$	$c_2\left(-\frac{3}{4} + \frac{\pi^2}{32} + \frac{\ln(2)}{2}\right)$
D_2^{add}	0	$-\frac{3}{4}c_2$	$c_2\left(-\frac{9}{4} - \frac{3\pi^2}{32} + \frac{13\ln(2)}{4}\right)$
D_3^z	0	0	$c_2\left(-\frac{1}{4} - \frac{\pi^2}{32} + \ln(2)\right)$
D_3^{add}	0	0	$c_2\left(\frac{1}{4} + \frac{3\pi^2}{32} - \frac{\ln(2)}{4}\right)$
D_4^z	0	$-\frac{1}{4}c_1$	$c_1\left(-\frac{1}{4} + \frac{\pi^2}{16}\right)$
D_4^{add}	0	$-\frac{1}{4}c_1$	$c_1\left(-\frac{1}{8} + \frac{\pi^2}{32} - \frac{\ln(2)}{2}\right)$
D_5^z	0	0	0
D_5^{add}	0	0	$c_1\left(\frac{1}{8} - \frac{\pi^2}{32} - \frac{\ln(2)}{2}\right)$
D_6^z	0	$\frac{5}{8}c_1$	$c_1\left(-\frac{1}{8} - \frac{\ln(2)}{4}\right)$
D_6^{add}	0	$\frac{13}{16}c_1$	$c_1\left(-\frac{1}{8} - \frac{\ln(2)}{8}\right)$
D_7^z	0	0	$c_1\frac{3}{8}$
D_7^{add}	0	$\frac{3}{16}c_1$	$c_1\left(-\frac{3}{8} + \frac{\ln(2)}{8}\right)$
D_8^z	0	$-\frac{1}{4}c_2$	$c_2\left(-\frac{1}{4} + \frac{\pi^2}{16} - \frac{\ln(2)}{2}\right)$
D_8^{add}	0	$-\frac{1}{4}c_2$	$c_2\left(\frac{1}{4} - \frac{\pi^2}{16} - \frac{3\ln(2)}{4}\right)$
D_9^z	0	0	0
D_9^{add}	0	0	$-c_2\frac{\ln(2)}{4}$
D_{10}^z	$\frac{1}{8}(c_1 - c_2)$	$-\frac{3}{8}(c_1 - c_2)$	$(c_1 - c_2)\left(\frac{1}{2} - \frac{\ln(2)}{2}\right)$
D_{10}^{add}	$-\frac{3}{8}(c_1 - c_2)$	$-\frac{3}{8}(c_1 - c_2)$	$-(c_1 - c_2)\left(\frac{1}{2} + \frac{3\ln(2)}{8}\right)$
D_{11}^z	0	0	0
D_{11}^{add}	0	0	$-(c_1 - c_2)\frac{3\ln(2)}{8}$

Table 2. Contributions to $\mathcal{I}_g(0)$ of $D_{12}, \ldots, D_{17}$ and the mass counterterm diagrams

Diagram	ϵ^{-1}	ϵ^{0}
$\left(D_{12} + C_1 \frac{\delta m}{m} + D_{14} + D_{16}\right)$	$-\frac{1}{4}(c_1 - c_2)$	$c_1\left(\frac{1}{2} + \frac{\ln(2)}{2}\right) - c_2\left(\frac{1}{4} + \frac{\ln(2)}{2}\right)$
$\left(D_{13} + C_3 \frac{\delta m}{m} + D_{15} + D_{17}\right)$	0	$-(c_1 - c_2)\frac{1}{4}$
$C_2^z \frac{\delta m}{m}$	$-\frac{3}{8}c_1$	$c_1\left(\frac{1}{8} + \frac{3\ln(2)}{4}\right)$
$C_2^{\text{add}} \frac{\delta m}{m}$	$-\frac{9}{16}c_1$	$c_1 \frac{9\ln(2)}{8}$
$C_4^z \frac{\delta m}{m}$	0	$-c_1 \frac{3}{8}$
$C_4^{\text{add}} \frac{\delta m}{m}$	$-\frac{3}{16}c_1$	$c_1\left(\frac{1}{4} + \frac{3\ln(2)}{8}\right)$

Results: Quark NLO CF

$$T_q(x,\xi) = \frac{\alpha_S^2(\mu_R)C_F}{2\pi} f_q\left(\frac{x-\xi+i\varepsilon}{2\xi}\right),$$

$$\begin{aligned} f_q(y) = {} & \ln\left(\frac{4m^2}{\mu_F^2}\right)(1+2y)\left(\frac{\ln(-y)}{1+y} - \frac{\ln(1+y)}{y}\right) - \pi^2\frac{13(1+2y)}{48y(1+y)} + \frac{2\ln 2}{1+2y} \\ & + \frac{\ln(-y)+\ln(1+y)}{1+2y} + (1+2y)\left(\frac{\ln^2(-y)}{1+y} - \frac{\ln^2(1+y)}{y}\right) \\ & + \frac{3-4y+16y(1+y)}{4y(1+y)} Li_2(1+2y) - \frac{7+4y+16y(1+y)}{4y(1+y)} Li_2(-1-2y) \end{aligned}$$

$y = \frac{x_1 s - M^2}{M^2} = \frac{x_2}{\zeta} = \frac{x-\xi}{2\xi}$ $\qquad$ $\zeta = \frac{M^2}{W^2}$

Results: Gluon NLO CF

$$T_g(x,\xi) = \frac{\xi}{(x-\xi+i\varepsilon)(x+\xi-i\varepsilon)}\left[\alpha_S(\mu_R) + \frac{\alpha_S^2(\mu_R)}{4\pi} f_g\left(\frac{x-\xi+i\varepsilon}{2\xi}\right)\right]$$

$$\begin{aligned}
f_g(y) &= 4(c_1-c_2)\big(1+2y(1+y)\big)\Big(\frac{\ln(-y)}{1+y} - \frac{\ln(1+y)}{y}\Big)\Big(\ln\frac{4m^2}{\mu_F^2} - 1\Big) + \beta_0 \ln\frac{\mu_R^2}{\mu_F^2} \\
&+ 4(c_1-c_2)\big(1+2y(1+y)\big)\left(\frac{\ln^2(-y)}{1+y} - \frac{\ln^2(1+y)}{y}\right) - 8c_1 \\
&- \pi^2\left(\frac{2+y(1+y)(25+88y(1+y))}{48y^2(1+y)^2}c_1 + \frac{10+y(1+y)(7-52y(1+y))}{24y^2(1+y)^2}c_2\right) \\
&- \left[c_1\frac{1+6y(1+y)(1+2y(1+y))}{y(1+y)(1+2y)^2} + c_2\frac{(1+2y)^2}{y(1+y)}\right]\ln(2) \\
&+ \pi\frac{\sqrt{-y(1+y)}}{y(1+y)}\left(\frac{7}{2}c_1 - 3c_2\right) \\
&+ 2c_2\frac{\sqrt{-y(1+y)}}{y(1+y)}\left(\frac{1+4y}{1+y}\arctan\sqrt{\frac{-y}{1+y}} + \frac{3+4y}{y}\arctan\sqrt{\frac{1+y}{-y}}\right) \\
&- \frac{\arctan^2\sqrt{\frac{-y}{1+y}}}{2y(1+y)}\left((7+4y)c_1 - 2\frac{1+2y-2y^2}{1+y}c_2\right) \\
&- \frac{\arctan^2\sqrt{\frac{1+y}{-y}}}{2y(1+y)}\left((3-4y)c_1 - 2\frac{3+6y+2y^2}{y}c_2\right) \\
&+ 2\,a_1(y)\ln(-y) + 2\,a_1(-1-y)\ln(1+y) \\
&+ 2\,a_2(y)Li_2(1+2y) + 2\,a_2(-1-y)Li_2(-1-2y)\,,
\end{aligned}$$

$$c_1 = C_F \qquad c_2 = C_F - \frac{C_A}{2} = -\frac{1}{2N_c}$$

Confrontation with data and phenomenology

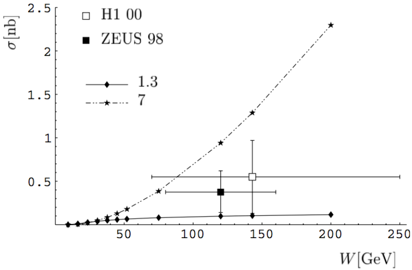

Fig. 13. The cross section for Υ photoproduction; the theoretical predictions at LO for the scales $\mu_F = \mu_R = [1.3, 7]$ GeV (ranging from bottom to top), and the data are from ZEUS [5] and H1 [6]

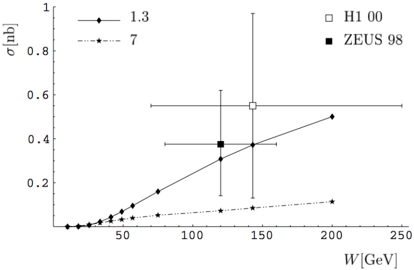

Fig. 14. The cross section of the Υ photoproduction; theoretical predictions at NLO for the scales $\mu_F = \mu_R = [1.3, 7]$ GeV (ranging from top to bottom), and the data from ZEUS [5] and H1 [6]

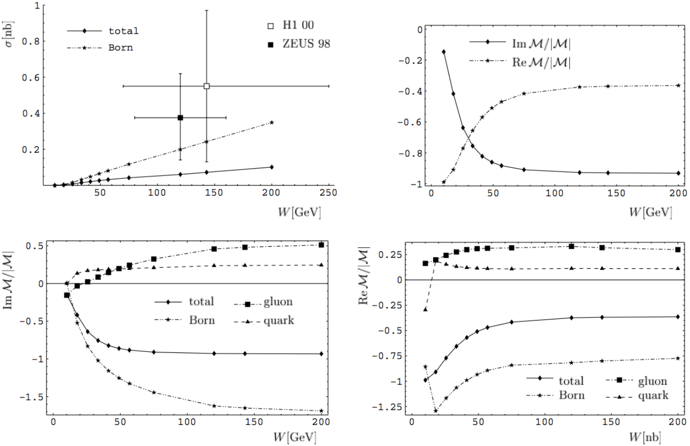

Fig. 15. Υ photoproduction, NLO prediction for $\mu_F = \mu_R = 4.9\,\text{GeV}$ and its decomposition into different contributions; s

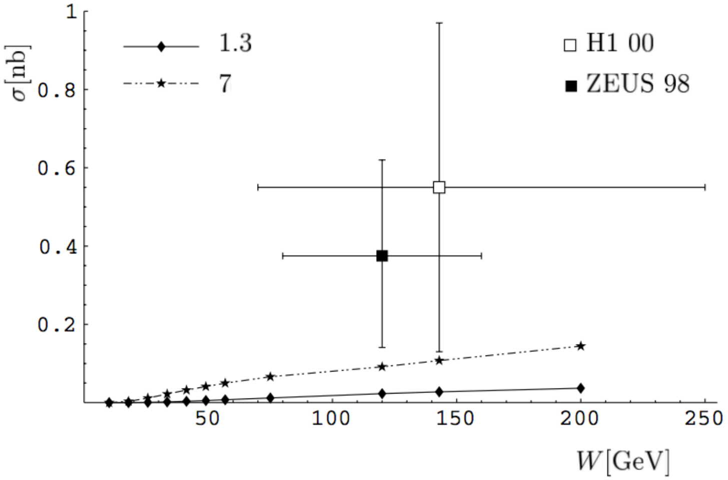

Fig. 16. The cross section for Υ photoproduction, and NLO predictions for the scales $\mu_F = [1.3, 7]\,\text{GeV}$, $\mu_R = 5.9\,\text{GeV}$

J/Ψ production

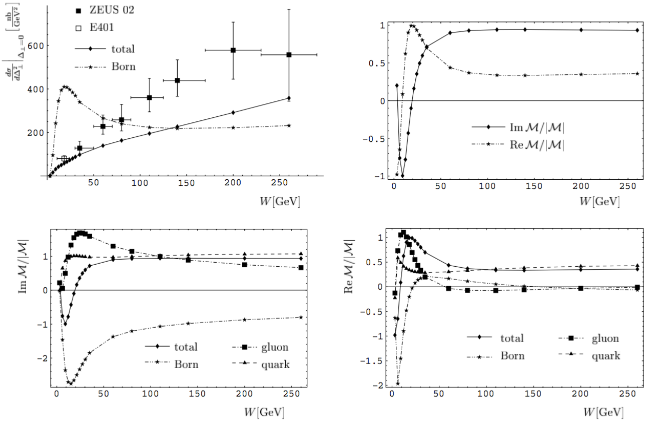

Fig. 17. The differential cross section for J/ψ photoproduction, NLO predictions for $\mu_F = \mu_R = 1.52\,\mathrm{GeV}$, and the data from E401 [1] and ZEUS [7]. The labeling of the curves is the same as in Fig. 15

Photoproduction cross section - LO and NLO

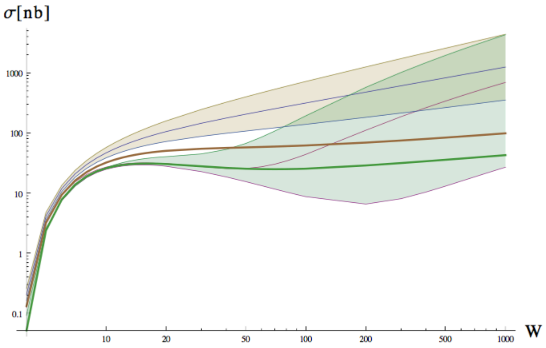

Figure : Photoproduction cross section as a function of $W = \sqrt{s_{\gamma p}}$ for $\mu_F^2 = M_{J/\psi}^2 \times \{0.5, 1, 2\}$- LO and NLO. Thick lines for LO and NLO for $\mu_F^2 = 1/4 M_{J/\psi}^2$.

- Jones & Martin & Ryskin & Teubner, arXiv:1507.06942. Choice of the factorization scale.
- Why NLO corrections are large at small x_B?
  large contribution comes from

$$ImA^g \sim H^g(\xi,\xi) + \frac{3\alpha_s}{\pi}\left[\log\frac{M_V^2}{\mu_F^2} - \log 4\right]\int_{\xi}^{1}\frac{dx}{x}H^g(x,\xi)$$

$H^g(x,\xi) \sim xg(x) \sim const$, therefore $\int dx/xH^g(x,\xi) \sim \log(1/\xi)H^g(\xi,\xi)$

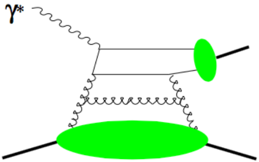

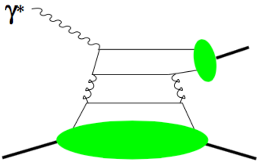

At higher orders powers of energy log are generated

$$\mathcal{I}m A^g \sim H^g(\xi,\xi) + \int\limits_{\xi}^{1} \frac{dx}{x} H^g(x,\xi) \sum_{n=1} C_n(L) \frac{\bar{\alpha}_s^n}{(n-1)!} \log^{n-1}\frac{x}{\xi}$$

$C_n(L)$ - polynomials of $L = \log\frac{Q^2}{\mu_F^2}$, maximum power is L^n

- for DIS a technique suggested by Catani, Ciafaloni and Hautmann; [Catani, Hautmann '94]
- One can calculate $C_n(L)$ in $D = 4 + 2\epsilon$ dimensions.
- Consistently with collinear factorization, in terms of corrections to coeff. functions and anomalous dimensions, in $\overline{MS}$ scheme
- The method used in DIS can be generalized to exclusive, nonforward processes.

Coeff. functions at small x / their Mellin moments at $N \to 0$

$$L = \log\left(\frac{Q^2}{\mu_F^2}\right) \quad , \quad x = \frac{\bar{\alpha}_s}{N}$$

Result for $J/\Psi, \Upsilon$

$$1 + x(L - \log 4) + \frac{x^2}{6}\left(\pi^2 + 3\log^2 4 + 3L(L - \log 16)\right) + \cdots + \mathcal{O}(x^{10})$$

F_L – [Catani, Hautmann '94]

$\mu_F^2 = Q^2$

F_L: $\quad 1 - \frac{1}{3}\,x + 2.13\,x^2 + 2.27\,x^3 + 0.434\,x^4 + \ldots$

$J/\Psi, \Upsilon$: $\quad 1 - 1.39\,x + 2.61\,x^2 + 0.481\,x^3 - 4.96\,x^4 + \ldots$

J. Wagner, Poetic 2015

Resummed amplitude for J/ψ

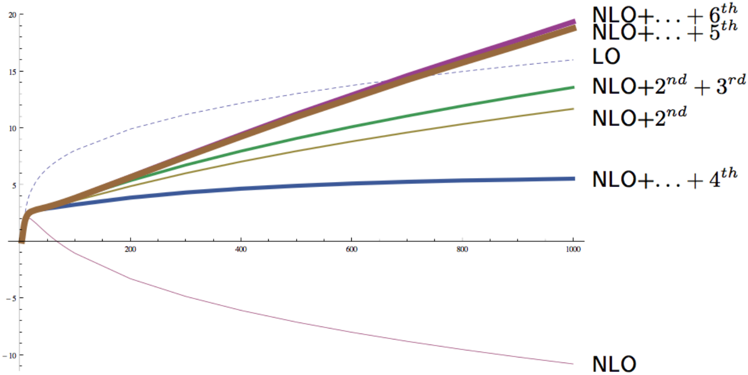

Imaginary part of the amplitude for photoproduction of heavy mesons as a function of $W = \sqrt{s_{\gamma p}}$ for $\mu_F^2 = M_{J/\psi}^2$

J. Wagner, Poetic 2015

Resummed cross section for J/ψ

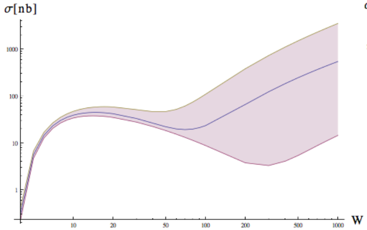

NLO

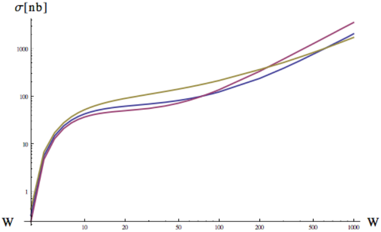

Resummed

Photoproduction cross section as a function of $W = \sqrt{s_{\gamma p}}$ for $\mu_F^2 = M_{J/\psi}^2 \times \{0.5, 1, 2\}$

Conclusions

- NLO calculations permit to check correctness of the all-order-proof of QCD factorisation

- NLO corrections are very important for quarkonia photoproduction

- High energy resummation needed for quarkonia photoproduction